Performance Evaluation of Full-Duplex Energy Harvesting Relaying Networks Using PDC Self-Interference Cancellation

Jiaman Li
School of Electrical, Computer and Telecommunication Engineering
University of Wollongong
jl797@uowmail.edu.au

Le Chung Tran
School of Electrical, Computer and Telecommunication Engineering
University of Wollongong
lctran@uow.edu.au

Farzad Safaei
School of Electrical, Computer and Telecommunication Engineering
University of Wollongong
farzad@uow.edu.au

***Abstract*—In this paper, throughput and bit error performance of an in-band full duplex (IBFD) relaying system assisted by the radio frequency energy harvesting technique and the polarization-enabled digital self-interference cancellation (PDC) scheme are investigated. In particular, the relay node harvests power from the wireless radio frequency signal transmitted from the source node and uses this power to amplify and forward signals to the destination. Meanwhile, the PDC scheme is used at the relay node to cancel the self-interference signal in order to facilitate the concurrent in-band transmission and reception. The impact of both energy harvesting and self-interference cancellation on the throughput and the error performance of the system is evaluated. Our simulation results show that the full-duplex energy harvesting relaying system almost doubles the system throughput, compared to the half-duplex energy harvesting relaying system, at the cost of about 5 dB inferior error performance, partially because of the noise effect of the PDC scheme. We also show that to achieve a high throughput along with a good error performance in the full-duplex energy harvesting relaying system, a combined selection of a high signal-to-noise ratio and a suitable energy harvesting time is required.**

Keywords—Full-duplex relaying, self-interference cancellation, energy harvesting, throughput, bit error rate.

I. INTRODUCTION

In a system where there is no direct link between the source node and the destination node, the assistance of other nodes is needed to forward information to the destination. Thus, relaying networks and their characteristics are important to investigate. Meanwhile, energy harvesting, which harvests energy from radio frequency (RF) electromagnetic radiation, has attracted a significant interest, since it prolongs the lifetime of wireless sensor nodes. For example, the work in [1], [2] investigates relaying systems with wireless energy harvesting. The relay node converts the energy from the source into its own energy to forward the signal to the destination, but the relay is limited to the half-duplex (HD) mechanism. In [3], a full-duplex (FD) relaying network is investigated, which allows simultaneous transmission and reception in the same frequency band. The network provides higher spectrum efficiency compared to time division duplex and frequency division duplex. However, this paper assumes a perfect self-interference cancellation mechanism, thus ignoring the influence of the self-interference cancellation circuitry. In a full-duplex relaying system, the signal received at the relay from the distant transmitter is referred to the desired signal, while the transmitted signal from the local relaying transmitter is the self-interference signal. Because transmission and reception in a full-duplex system occur at the same time and in the same frequency band, the self-interference signal is mixed with the desired signal, leading to a signal corruption at the receiver of the relay. Thus, it is crucial that the self-interference signal is suppressed in the relay node before the desired signal is amplified and forwarded to the destination. By now many techniques to suppress self-interference signals have been researched. In the pioneering work by Everett et al. [4], passive self-interference cancellations, including directional isolation, absorptive shielding and cross-polarization, are studied. Besides, self-interference techniques in the RF domain for different transmission bandwidths are investigated in [5–9]. In the digital domain, self-interference techniques to handle residual self-interference after the analog-to-digital converter are considered in [10–12]. Most of the existing cancellation methods depend on the reconstruction of the self-interference (SI) signal and then subtracting it from the received signal to extract the desired signal. In contrast, the polarization-enabled digital self-interference cancellation (PDC) scheme proposed by Liu et al. [13] distinguishes the self-interference signal from the desired signal in the polarized domain and cancels the self-interference using an oblique projection. However, this proposal does not consider the energy harvesting mechanism and is not applied to relaying systems. To the best of our knowledge, no works, especially in the polarized domain, have considered the performance of self-interference cancellation methods in the full-duplex relaying system with RF energy harvesting. Given that both full-duplex communications and RF energy harvesting are important emerging technologies for 5G systems, performance evaluation of full-duplex energy harvesting relaying networks is of considerable importance. This is the motivation of our paper.

In this paper, we consider a dual-hop full-duplex relaying system, where the relaying node harvests the RF energy from the source node, then uses this energy to amplify and forward the signal to the destination. We assume there is no direct link between the source node and the destination node. Thus, the relay is used to assist the transmission from the source to the destination. We also assume that the time switching method [3], [14] is used at the relay to harvest the RF energy and the PDC scheme is used to cancel self-interference at the relay.

The main contributions of the paper are summarized as follow:

- We investigate the throughput of an in-band full-duplex relaying system assisted by RF energy harvesting and the PDC self-interference cancellation. We consider the throughput based on the fraction of time α used to harvest energy for a

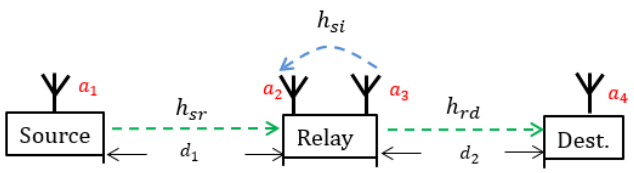

Fig. 1. Full-duplex relaying system model

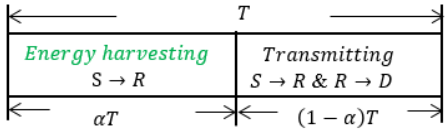

Fig. 2. Full-duplex TSR protocol for energy harvesting and information processing

range of SNR and modulation methods. We show that the maximum throughput appears at a lower range of α values for a higher SNR, while this optimal α is invariant for different modulation methods. This observation means that, to achieve a high throughput, a joint combination of a high SNR value and a low α value is expected.

- We examine the system bit error rate (BER) performance under the impacts of RF energy harvesting and the PDC self-interference cancellation. It is revealed that, for the same SNR, the BER performance of the system only improves slightly when α increases. Combined with the above observation, this result means that the energy harvesting scheme can be optimized to improve significantly the system throughput without impacting the BER performance of the PDC self-interference cancellation scheme.
- We quantify the impact of the energy harvesting and PDC scheme on the BER performance in comparison with the half-duplex energy harvesting relaying system. Our results show that the PDC scheme can effectively cancel the self-interference in the full-duplex system at the cost of a slight increase of noise. In particular, if the relay transmission power (per symbol) is the same in both full-duplex and half-duplex systems, the BER performance curve of the former is within 2 dB inferior compared to that of the latter. Thus, applying the PDC cancellation scheme to achieve a high throughput and reasonable BER for our full-duplex energy harvesting relaying systems seems feasible.

The rest of paper is organized as follows. In Section Ⅱ, the system model is presented. In Section Ⅲ, the signal model for the polarization-enabled digital self-interference cancellation scheme is described. The simulation results and performance analysis are presented in Section Ⅳ. Section Ⅴ concludes the paper.

II. System Model

In this paper, the dual-hop in-band full-duplex relaying system with energy harvesting at the relay node is considered. We assume that there is no direct link between the source node and the destination node. Thus, an intermediate relay is used to assist the transmission from the source to the destination as shown in Fig. 1. The system has a single source node, a relay node, and a destination node. Denote a_1 to a_4 as orthogonally dual-polarized antennas, in which the antennas a_1 and a_3 are used for transmission, while a_2 and a_4 are used for reception. The flat-fading channel gains from the source to the relay and from the relay to the destination are denoted as h_{sr} and h_{rd}, and the distances between them are presented as d_1 and d_2 respectively. As the system is a full duplex one, the relay is able to receive signals from the source while transmitting signals to the destination at the same time in the same frequency band. Thus the local transmit antenna a_3 generates self-interference (SI) signals in the same frequency band, which will be mixed with the desired signal at the receive antenna a_2. Denote h_{si} as the propagation coefficient of the SI channel which is assumed to follow a Rayleigh distribution. The PDC scheme [13] is applied at the relay to cancel self-interference signals.

In addition, the relay node is equipped with the time switching-based relaying (TSR) protocol [3], [14] for energy harvesting and information processing. The full-duplex TSR protocol is depicted in Fig. 2. The whole signal block lasting T (seconds) is divided into an energy harvesting section and an information transmitting section. We define α, where $0 < \alpha < 1$, as the fraction of time in which the relay harvests the energy from its received signals. Thus, αT time is used for the energy harvesting and the remaining block time (1-α)T is used to transmit the desired signal in a full-duplex transmission mode. The intermediate relay harvests energy from the RF signal transmitted from the source within the duration αT. We assume that energy harvesting is carried out without any limit on the minimum power level of the received RF signal. Then, the relay uses the harvested energy as a source of transmitting power to amplify and forward the source information to the destination within the duration (1-α)T. Besides, the PDC scheme is activated during this period to cancel the SI signal. After SI cancellation, the resulting signal is amplified by the relay before being forwarded to the destination. Finally, the received signal at the destination is detected by the maximum ratio combining (MRC) method.

III. Signal Model

Define $x(n)$ and $z(n)$ as the desired signal from the source and the self-interference signal from the relay transmitter at the time instant n, respectively. Define $n_r(n)$ as the additive white Gaussian noise at the relay with the variance of σ^2. Denote m as the path loss exponent, P_s as the source transmit power, and P_i as the interference power at the receive antenna of the relay. The channel coefficients are presented in Fig.1. Then, in a conventional non-polarized full-duplex system, the received temporal signal $y_r(n)$ at the relay is

$$y_r(n) = \left(\frac{1}{\sqrt{d_1^m}}\right)\sqrt{P_s}\, h_{sr}\, x(n) + \sqrt{P_i}\, h_{si}\, z(n) + n_r(n) \quad (1)$$

However, in this paper, since the orthogonally dual-polarized antennas are used to transmit and receive the polarized signals, the relay receives the polarized signals, each of which has a horizontally polarized component (H) and a vertically polarized component (V). Denote the polarization states (PS) of the desired signal and self-interference signal as **S** and **I** respectively. The bold letters in this paper represent vectors.

$$\mathbf{I} = [\cos(\varepsilon_i) \quad \sin(\varepsilon_i)\exp(j\delta_i)]^T = [H_i \quad V_i]^T \tag{2}$$

$$\mathbf{S} = [\cos(\varepsilon_s) \quad \sin(\varepsilon_s)\exp(j\delta_s)]^T = [H_s \quad V_s]^T \tag{3}$$

where $\varepsilon_{i/s} \in [0,\pi/2]$ is the polarized angle and $\delta_{i/s} \in [0,2\pi]$ describes the phase difference between the horizontal polarized component and the vertical polarized one. Clearly, $\mathbf{S}$ and $\mathbf{I}$ are unit vectors, i.e., $\mathbf{S}^H\mathbf{S} = 1$ and $\mathbf{I}^H\mathbf{I} = 1$, where $(.)^T$ represents transpose and $(.)^H$ represents Hermitian transposition. Thus, in the polarized system, the polarized received signal at the relay node, namely the input signal of the PDC scheme, can be written as

$$\mathbf{Y}(n) = \mathbf{X}(n) + \mathbf{Z}(n) + \mathbf{N}(n)$$

$$= \left(\frac{1}{\sqrt{d_1^m}}\right)\sqrt{P_s}\, h_{sr}\, \mathbf{S}\, x(n) + \sqrt{P_i}\, h_{si}\, \mathbf{I}\, z(n) + \begin{bmatrix} n_H \\ n_V \end{bmatrix} \tag{4}$$

where n_H is the horizontal component of $n_r(n)$ and n_V is its vertical component. The component n_H and n_V are independent complex Gaussian random variables with zero mean and the variance of $\sigma^2/2$.

The signal $\mathbf{Y}(n)$ is then processed by the PDC scheme. The PDC scheme has two steps, namely oblique projection and scalarization. The objective of the oblique projection is to cancel the self-interference. The scalarization aims to transform a signal vector to a scalar form. The oblique projection operator $\mathbf{Q}_{SI}$ is derived as [13]

$$\mathbf{Q}_{SI} = [\mathbf{S}\ \mathbf{0}] \begin{bmatrix} \mathbf{S}^H\mathbf{S} & \mathbf{S}^H\mathbf{I} \\ \mathbf{I}^H\mathbf{S} & \mathbf{I}^H\mathbf{I} \end{bmatrix}^+ \begin{bmatrix} \mathbf{S}^H \\ \mathbf{I}^H \end{bmatrix} = \mathbf{S}(\mathbf{S}^H\mathbf{P}_I^+\mathbf{S})^{-1}\mathbf{S}^H\mathbf{P}_I^+ \tag{5}$$

where $\mathbf{P}_I^+ = \mathbf{E} - \mathbf{I}\,(\mathbf{I}^H\,\mathbf{I})^{-1}\,\mathbf{I}^H$, $(.)^+$ represents pseudo-inverse, $\mathbf{E}$ represents an identity matrix, and $\mathbf{0}$ is a zero vector. It is proved in [13] that $\mathbf{Q}_{SI}$ has the property of

$$\mathbf{Q}_{SI}\,[\mathbf{S}, \mathbf{I}] = [\mathbf{S}\ \mathbf{0}] \tag{6}$$

Thus,

$$\mathbf{Q}_{SI}\,\mathbf{Y}(n) = \mathbf{Q}_{SI}\,(\mathbf{X}(n) + \mathbf{Z}(n) + \mathbf{N}(n))$$

$$= \mathbf{Q}_{SI}\left[\left(\frac{1}{\sqrt{d_1^m}}\right)\sqrt{P_s}\, h_{sr}\, \mathbf{S}\, x(n) + \sqrt{P_i}\, h_{si}\, \mathbf{I}\, z(n) + \mathbf{N}(n)\right]$$

$$= \left(\frac{1}{\sqrt{d_1^m}}\right)\sqrt{P_s}\, h_{sr}\, \mathbf{S}\, x(n) + \mathbf{Q}_{SI}\,\mathbf{N}(n) \tag{7}$$

In order to transform the polarization vector to the scalar form, both sides of (7) are multiplied with $\mathbf{S}^H$ and note that $\mathbf{S}^H\mathbf{S} = 1$. The output signal $y(n)$ of the PDC scheme is

$$y(n) = \mathbf{S}^H\,(\mathbf{Q}_{SI}\,\mathbf{Y}(n))$$

$$= \left(\frac{1}{\sqrt{d_1^m}}\right)\sqrt{P_s}\, h_{sr}\, x(n) + \mathbf{S}^H\,\mathbf{Q}_{SI}\,\mathbf{N}(n) \tag{8}$$

Then, the signal $y(n)$ is amplified and forwarded by the relay node to the destination. Since the relay node is powered by the energy harvesting technique, the transmission power P_r of the relay node depends on the energy harvesting time αT and the source transmission power P_s. Denote the unit-power signal transmitted from the source node as $s_e(n)$, the received signal $y_e(n)$ at the relay during the harvesting time is

$$y_e(n) = \left(\frac{1}{\sqrt{d_1^m}}\right)\sqrt{P_s}\, h_{sr}\, s_e(n) + n_r(n) \tag{9}$$

Hence, using (9), the harvested energy at the relay within duration αT can be expressed as

$$E_r = \eta\alpha T\left(\frac{P_s\,|h_{sr}|^2}{d_1^m} + \sigma_p^2\right) \tag{10}$$

where $0 < \eta < 1$ is the energy conversion efficiency and σ_p^2 is the variance of the noise $\mathbf{S}^H\,\mathbf{Q}_{SI}\mathbf{N}(n)$ in (8).

The transmit power P_r of the relay in the remaining duration $(1-\alpha)T$ in the full-duplex system is calculated as

$$P_r = \frac{E_r}{(1-\alpha)T} = \frac{\eta\alpha}{(1-\alpha)}\left(\frac{P_s\,|h_{sr}|^2}{d_1^m} + \sigma_p^2\right) \tag{11}$$

The PDC output signal $y(n)$ in Eq. (8) is amplified to the power P_r by the relay. The transmitted signal at the relay $x_r(n)$ is

$$x_r(n) = \frac{\sqrt{P_r}\, y(n)}{\sqrt{\frac{P_s|h_{sr}|^2}{d_1^m} + \sigma_p^2}}$$

$$= \sqrt{\frac{\eta\alpha P_s}{(1-\alpha)d_1^m}}\ h_{sr}\, x(n) + \sqrt{\frac{\eta\alpha}{(1-\alpha)}}\ \mathbf{S}^H\,\mathbf{Q}_{SI}\,\mathbf{N}(n) \tag{12}$$

The received signal $y_d(n)$ at the destination is

$$y_d(n) = \left(\frac{1}{\sqrt{d_2^m}}\right) h_{rd}\, x_r(n) + n_d(n)$$

$$= \sqrt{\frac{\eta\alpha P_s}{(1-\alpha)d_1^m d_2^m}}\ h_{sr}\, h_{rd}\, x(n)$$

$$+ \sqrt{\frac{\eta\alpha}{(1-\alpha)d_2^m}}\ h_{rd}\, \mathbf{S}^H\,\mathbf{Q}_{SI}\,\mathbf{N}(n) + n_d(n) \tag{13}$$

where $n_d(n)$ is the AWGN at the destination with the variance of σ^2.

The signal $y_d(n)$ is then processed by the maximum ratio combining (MRC) detection method. Denote $(.)^*$ as the complex conjugate, the resulting signal $y_{de}(n)$ used for demodulation is

$$y_{de}(n) = h_{sr}^*\, h_{rd}^*\, y_d(n)$$

$$= h_{sr}^*\, h_{rd}^*\left[\sqrt{\frac{\eta\alpha P_s}{(1-\alpha)d_1^m d_2^m}}\ h_{sr}\, h_{rd}\, x(n)\right]$$

$$+ h_{sr}^*\, h_{rd}^*\left[\sqrt{\frac{\eta\alpha}{(1-\alpha)d_2^m}}\, h_{rd}\, \mathbf{S}^H\mathbf{Q}_{SI}\mathbf{N}(n) + n_d(n)\right] \tag{14}$$

IV. Simulation Results

In this section, simulation results are presented to reveal the throughput and BER performances of both half-duplex harvesting relaying system and full-duplex energy harvesting relaying system. In Part A, we investigate the impact of SNR and modulation scheme on the system throughput when the

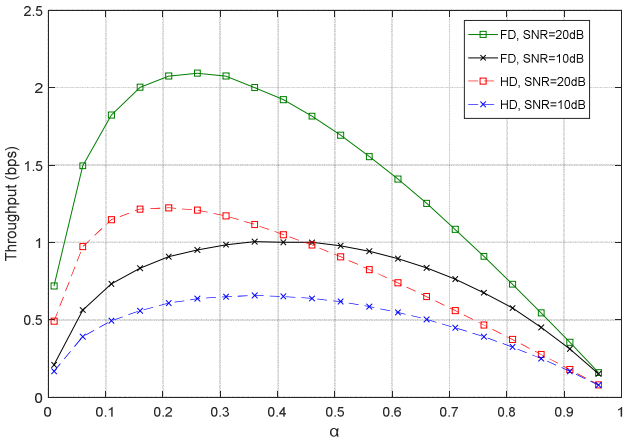

Fig. 3. Throughput comparison of half-duplex energy harvesting relaying system and full-duplex energy harvesting relaying system using QPSK modulation.

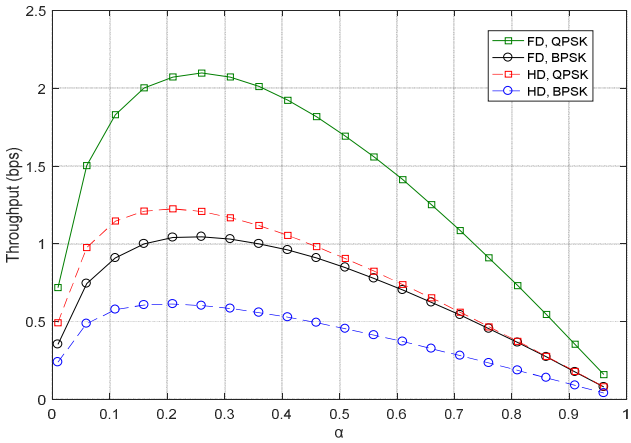

Fig. 4. Throughput comparison between BPSK and QPSK modulations for SNR = 20 dB.

value of α is varied. In Part B, we investigate the impact of the fraction of time α and modulation scheme on the BER with the change of SNR from 0 dB to 40 dB. P_s and P_r present the source and the relay transmission powers, respectively. The source transmission rate is set as R_1 = 2 bps for BPSK modulation and R_2 = 4 bps for QPSK modulation, hence, the total numbers of transmitted symbols in both BPSK and QPSK cases are the same. We set the corresponding outage SNR threshold to achieve the desired transmission rates R_1 and R_2 as $\gamma_{th1} = 2^{R_1} - 1 = 3$ and $\gamma_{th2} = 2^{R_2} - 1 = 7$, respectively. The path loss exponent is m = 4, the source-relay distance d_1 and relay-destination distance d_2 are 1 meter, and the energy harvesting efficiency is set to be η = 1 [1], [2]. Besides, we assume that the signal channel and the self-interference channel satisfy Rayleigh flat fading.

A. Throughput performances

The system outage probability can be calculated as

$$p_{out} = p(\gamma < \gamma_{th}) \tag{15}$$

where γ is the instantaneous SNR per symbol of the received signal at the destination and γ_{th} is the SNR threshold. Specifically, the threshold of BPSK modulation is γ_{th1} while that of QPSK modulation is γ_{th2}. The system throughput Thr can be calculated as

$$\text{Thr} = (1 - p_{out})\, R\, (1 - \alpha) \tag{16}$$

where R is the transmission rate. Recall that the transmission rate of BPSK modulation is R_1 while that of the QPSK modulation is R_2. The simulation results of the throughput are shown in Figs. 3 and 4.

Fig. 3 illustrates the throughput of both half-duplex (HD) and full-duplex (FD) relaying systems for different values of α. In both systems, the relay node is powered by the energy harvesting technique and the modulation scheme is QPSK. From Fig. 3, we have three observations. Firstly, a continuous increase of α is not necessary to improve the system throughput. For the four different scenarios in Fig. 3, the throughput curves are convex, i.e., the throughput reaches its maximum value at a certain α. This is because the system throughput Thr is a function of both p_{out} and (1-α) as shown in Eq. (18). Any increase in α results in a larger transmission power P_r of the relay, i.e., a smaller outage probability p_{out}, but also a shorter time duration (1-α)T used for transmission of information. For a small value of α, the throughput depends more on p_{out}, while it depends more on (1-α) when α becomes larger. Secondly, for different values of SNR, the throughput of the FD system in all case is around 1.6 times of the HD case. The reason is that although FD carries a doubled amount of symbols compared to HD during (1-α)T time, the total harvested energy during the αT time for relay transmission is the same. This means the relay transmission powers per symbol P_r of FD is half of HD, which decrease the throughput by 0.4 times. Thirdly, when SNR is larger, the maximum throughput appears at a lower α value. For example, at SNR = 20 dB, the throughput is peaked at around α = 0.18, while for SNR = 10 dB, it is maximum at α = 0.33. The reason is that, for the same transmission rate R, the throughput is a function of both p_{out} and α. The maximum throughput appears at the intersection of the two curves representing 1-p_{out} and R(1-α). When SNR increases, the function R(1-α) is unchanged while 1- p_{out} increases. This results in the intersection point of two curves to be shifted to the left-hand side. Thus, the maximum throughput appears at a lower α value.

Fig. 4 compares the throughputs for BPSK and QPSK modulations at SNR = 20 dB, which shows that the QPSK modulation significantly improves the throughput, compared to the BPSK modulation. The optimal α value for achieving the maximum throughput is invariant for these two modulation methods. Besides, the modulation method also has an influence on the BER performance as detailed in the following section.

B. Bit error rate

In this subsection, we examine the influence of modulation scheme and α on BER of the energy harvesting full-duplex system. We quantify the self-interference cancellation performance of the PDC scheme in the FD system and compare it with the HD system.

Fig. 5 compares the BER for BPSK and QPSK modulation schemes. The result shows that BPSK is superior to QPSK and the difference between them is about 3 dB in both HD and FD systems. This is because in our energy harvesting system, the relay transmission power per symbol is same, thus power per bit of BPSK is double that of QPSK while the Euclidean distance between the two nearest

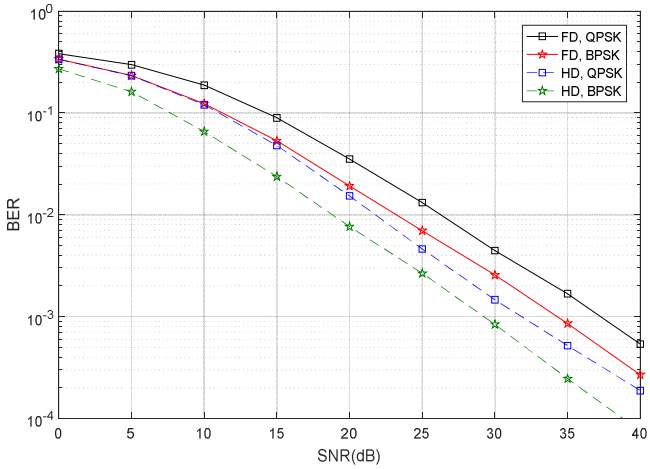

Fig. 5. Half-duplex energy harvesting relaying system vs. full-duplex energy harvesting relaying system associated with PDC for α = 0.2.

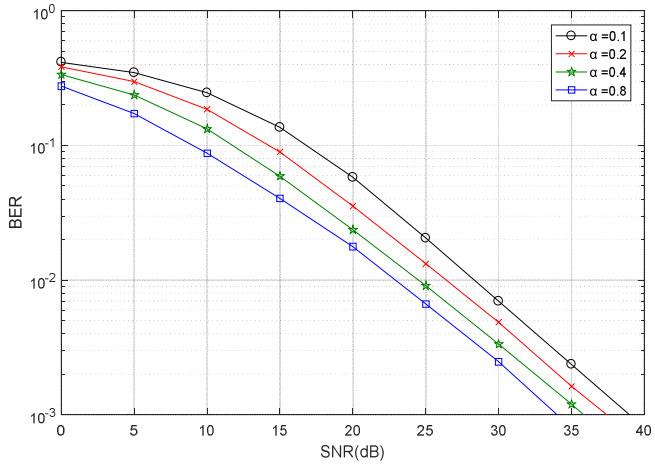

Fig. 6. Influence of α on BER of full-duplex energy harvesting relaying system using QPSK.

constellation points is $\sqrt{2}$ times that in QPSK. Fig. 5 also compares the BER of a half-duplex energy harvesting relaying system and that of a full-duplex energy harvesting relaying one with α = 0.2. As mentioned in Section VI.A, α = 0.2 can provide a large throughput but a low harvested energy. Within the αT time duration, the total harvested energy of HD and FD systems are equal, but in the information transmission period (1-α)T, the number of the transmitted information bits is doubled for the FD scenario, compared to the HD one. This means that the transmission power per bit at the relay of the FD system is half that in the HD one. Thus, although the BER performance curve of the FD system is 5 dB inferior to that of the HD one, 3 dB of its inferiority is accounted by the less relay transmission power per bit. Equivalently, the BER curve of the FD system is only 2 dB inferior to that of the HD one if the two powers are equal. This 2 dB inferiority is due to the additional noise introduced by the imperfect cancellation of the PDC scheme which is amplified by the relay as shown in the second part of Eq. (13). From Eq. (8), the PDC scheme can achieve a BER around 10^{-4} for BPSK and 10^{-3} for QPSK modulation at SNR = 40 dB. Without the PDC scheme, the desired signal cannot be detected as it is seriously corrupted by the self-interference signal. However, the side effect of the PDC scheme is the resulting noise as discussed before.

Fig. 6 examines the impact of the time fraction α on BER of the full-duplex energy harvesting relaying system using QPSK modulation. The value of α decides the total harvested energy. As α increases, the time αT used for energy harvesting increases while the total number of transmitted symbols with the duration (1-α)T decreases. This results in the increase of the relay transmission power per symbol. Thus, the increment of α decreases the system BER. When α is getting larger, especially when α > 0.5, BER continues to be improved, but the additional BER improvement becomes smaller. Besides, the increase of SNR improves the BER. At a high SNR value, e.g., SNR = 40 dB, BER can reach 10^{-3} even with α being as small as 0.1.

We recall from Figs. 3 and 4 that, the system throughput is high when α is in the lower half of its range; a higher value of SNR leads to a higher system throughput for all values of α and when SNR increases, the maximum throughput appears at a lower α value. From Figs. 5 and 6, when SNR increases, the BER decreases. These observations suggest that if we want to achieve a relatively high throughput along with a low BER in a full-duplex energy harvesting relaying system, a joint combination of a high SNR value and a low α value is expected.

V. Conclusion

In this paper, we considered an in-band full-duplex relaying system where the relay node harvests the RF energy from the source node to amplify and forward the signals. The relay node also uses the PDC scheme to cancel the SI signal. Our simulation results show that the energy harvesting mechanism has an influence on the system throughput and the cancellation performance of the PDC scheme. A full-duplex energy harvesting relaying system using the PDC can almost double the system throughput of a half-duplex energy harvesting relaying one. However, this high throughput in the FD system come at the cost of an inferior BER performance due to the characteristic of our energy harvesting system that the full-duplex system uses the same harvested energy as in the HD one to transmit doubled amount of information. The error performance inferiority is partially because of the additional noise introduced by the PDC scheme. A relatively good performance from both throughput and BER performance perspectives can be achieved in the full-duplex system by jointly optimizing SNR and α. For example, for the case of medium or high SNR, the value of α should be in its lower range. This paper has addressed the independent flat fading channels and a single antenna system. Our further work would be the generalization of this paper to address correlated fading channels [15], multipath (i.e., frequency selective fading) channels, and multi-antenna relaying networks.

References

[1] A. A. Nasir, X. Zhou, S. Durrani, and R. A. Kennedy, "Relaying protocols for wireless energy harvesting and information processing," *IEEE Trans. Wireless Commun.*, vol. 12, no. 7, pp. 3622-3636, Jul. 2013.

[2] K. M. Rabie, A. Salem, E. Alsusa, and M. S. Alouini, "Energy-harvesting in cooperative AF relaying networks over log-normal fading channels," in *IEEE Int. Conf. Commun. (ICC 2016),* May 2016, pp.1-7.

[3] C. Zhong, H. A. Suraweera, G. Zheng, I. Krikidis, and Z. Zhang, “Wireless information and power transfer with full duplex relaying," *IEEE Trans. Commun.*, vol. 62, no. 10, pp. 3447-461, Oct. 2014.

[4] E. Everett, A. Sahai, and A. Sabharwal, “Passive self-interference suppression for full-duplex infrastructure nodes," *IEEE Trans. Wireless Commun.*, vol. 13, no. 2, Feb. 2014.

[5] J. Tamminen et al., “Digitally-controlled RF self-interference canceller for full-duplex radios," in *24th European Signal Process. Conf. (EUSIPCO 2016)*, Aug. 2016, pp. 783-787.

[6] A. T. Le, L. C. Tran, and X. Huang, “Cyclostationary Analysis of Analog Least Mean Square Loop for Self-Interference Cancellation in In-Band Full-Duplex Systems”, *IEEE Commun. Lett.*, vol. 21, no. 12, pp. 2738-2741, Sep. 2017.

[7] A. T. Le *et al*., “Analog Least Mean Square Loop for Self-Interference Cancellation in Generalized Continuous Wave SAR”, in *88th IEEE Veh. Technol. Conf. (VTC-Fall 2018)*, Chicago, USA, Aug. 2018.

[8] A. T. Le, L. C. Tran, and X. Huang, “On performance of analog least mean square loop for self-interference cancellation in in-band full-duplex OFDM systems”, in *IEEE Veh. Technol. Conf. (VTC-Spring 2017)*, Sydney, Australia, Jun. 2017, pp. 1-5.

[9] A. T. Le, L. C. Tran, X. Huang, Y. J. Guo and J. Y. Vardaxoglou, "Frequency Domain Characterization and Performance Bounds of ALMS Loop for RF Self-Interference Cancellation," *IEEE Trans. Commun.*.

[10] D. Korpi *et al*., “Digital self-interference cancellation under nonideal RF components: Advanced algorithms and measured performance," in *16th IEEE International Workshop on Signal Processing Advances in Wireless Communications (SPAWC 2015),* Jun. 2015, pp. 286-290.

[11] M. Duarte and A. Sabharwal, "Full-duplex wireless communications using off-the-shelf radios: Feasibility and first results," in *44th Asilomar Conference on Signals, Systems and Computers (ASILOMAR 2010)*, Nov. 2010, pp. 1558-1562.

[12] D. Korpi *et al*., "Adaptive nonlinear digital self-Interference cancellation for mobile inband full-duplex radio: Algorithms and RF measurements," in *IEEE Global Communications Conference (GLOBECOM 2015)*, Dec. 2015, pp. 1-7.

[13] Y. Liu, C. Guo, Z. Zeng, and D. Li, “The polarization-enabled digital self-interference cancellation scheme for the full duplex communication," in *International Symposium on Wireless Personal Multimedia Communications (WPMC 2014)*, Sep. 2014, pp. 414-418.

[14] J. Feng, S. Ma, G. Yang and B. Xia, "Wireless information and power transfer in full-duplex two-way massive MIMO AF relay systems," in *IEEE 85th Vehicular Technology Conference (VTC Spring 2017),* Jun. 2017, pp. 1-5.

[15] L. C. Tran, T. A. Wyocki, A. Mertins, and J. Seberry, “A generalized algorithm for the generation of correlated Rayleigh fading envelopes in wireless channels,” *EURASIP J. Wireless Commun. Netw.*, vol. 2005, no. 5, pp. 801–815, Dec. 2005.